



ORIGINAL ARTICLE | DOI: 10.5584/jiomics.v1i2.56

## The effect of $Zn^{2+}$ on prostatic cell cytotoxicity caused by *Trichomonas vaginalis*

Laura Isabel Vazquez-Carrillo<sup>1</sup>, Laura Itzel Quintas-Granados<sup>1</sup>, Rossana Arroyo<sup>2</sup>, Guillermo Mendoza Hernández<sup>3</sup>, Arturo González-Robles<sup>2</sup>, Bertha Isabel Carvajal-Gamez<sup>1</sup>, M. Elizabeth Álvarez-Sánchez<sup>1</sup>

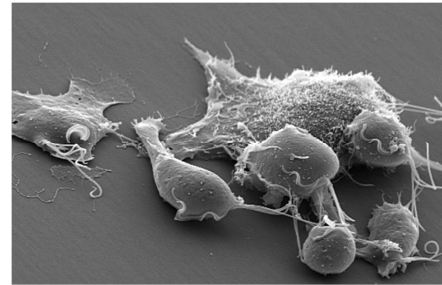
<sup>1</sup>Posgrado en Ciencias Genómicas, Universidad Autónoma de la Ciudad de México, plantel del Valle, San Lorenzo #290 Col. Del Valle, CP 03100 México DF, México. Telephone: +52 36912000 x 15306. Fax number: +52 55755805; <sup>2</sup>Departamento de Infectómica y Patogénesis Molecular, Centro de Investigación y de Estudios Avanzados del Instituto Politécnico Nacional; <sup>3</sup>Departamento de Bioquímica, Facultad de Medicina, Universidad Nacional Autónoma de México, México, D.F., México.

Received: 1 December 2010 Accepted: 3 February 2011 Available Online: 15 February 2011

### ABSTRACT

Our investigation focused on the study of the proteome, morphology, and cytotoxicity of *T. vaginalis* during interactions with prostatic DU-145 cells. The results suggest that approximately 37 different proteins are expressed in the presence of  $Zn^{2+}$ , which also down-regulates the protein and transcriptional levels of TvCP65. The result is a negative effect on trichomonal cytotoxicity. The differentially expressed proteins were identified by mass spectrometry analysis.

**Keywords:** *Trichomonas vaginalis*; DU-145 prostatic cells; morphology;  $Zn^{2+}$  proteome; cytotoxicity; TvCP65.



### 1. Introduction

*Trichomonas vaginalis* is the causative agent of trichomoniasis, a common worldwide infection associated with important public health problems [1] and implicated as a cofactor in the transmission of the human immunodeficiency virus [2]. This infection causes infertility [3], low birth weight infants and preterm delivery [4], and a predisposition to cervical neoplasia [5]. Infections in women cause vaginitis, cervicitis, urethritis, a malodorous seropurulent vaginal discharge and infertility [3, 6]. The cytopathogenicity of *T. vaginalis* begins with cytoadherence to target cells, which is mediated by ligand-receptor type interactions [7-8]. After adherence to vaginal epithelial cells (VECs), *T. vaginalis* suffers a dramatic change from ellipsoid to amoeboid [9]. Five adhesins (AP65, AP51, AP33, AP23, and AP120) [10-12] and two cysteine proteinases (CPs) (TvCP30 and TvCP62) [1, 13-15] participate in trichomonal adherence. Following adherence, a cytotoxic effect on the VECs cells, due to two CPs

(TvCP65, 65 kDa, [16-17] and TvCP39, 39 kDa, [18-19]), is observed before the target cells are phagocytized by the parasite [20]. In addition, other processes are involved in host colonization and target cell damage, such as hemolysis [21], immune evasion [22-23], signal transduction [9], and apoptosis induction [24].

Studies about female trichomoniasis indicate that iron ( $Fe^{2+}$ ), which is a component of the vaginal microenvironment, is also an essential element up-regulating numerous trichomonad genes. The  $Fe^{2+}$  concentration in the female microenvironment changes during the menstrual cycle, which modulates the expression of crucial metabolic enzymes and several pathogenic properties, and also leads to the multiplication and cytoadherence of *T. vaginalis* [25]. Not only is adhesin synthesis positively regulated by  $Fe^{2+}$  [26], but some proteinases involved in C3b complement component degradation [22] and immune evasion through the regulation of

\*Corresponding author: Elizabeth Álvarez-Sánchez. Email Address: elizabethalvarezsanchez@yahoo.com.mx.

P270 phosphorylation [27] are also regulated by this cation. Furthermore,  $\text{Fe}^{2+}$  down-regulates proteinases involved in trichomonal cytotoxicity, TvCP65 and TvCP39, which also participate in the interaction between the parasite and host, e.g., HeLa cells and VECs [1, 18]. In particular, TvCP65 degrades collagen IV and fibronectin in a broad pH range [16]. In contrast, TvCP39 degrades collagens (I, III, IV, and V), fibronectin and hemoglobin, and human IgA and IgG [18]. Interestingly, the proteolytic activities of TvCP39 [19] and TvCP65 [28] are negatively regulated by  $\text{Fe}^{2+}$ , the transcript and protein expression levels of TvCP65 agree with this decreased proteolytic activity [28].

Although trichomoniasis affects men, most are asymptomatic [29]. However, mild cases of urethritis, chronic prostatitis, and epididymitis have been associated with this infection [30]. *T. vaginalis* has several consequences in men's health, such as reduced sperm cell motility due to cell surface interactions between the parasite and the head or tail of the sperm as well as due to the flagella of parasites [31], which leads to male infertility [32]. During male infections, *T. vaginalis* accesses the microenvironment of the prostate, which is the gland that surrounds the posterior urethra of a man and, along with the seminal vesicles, produces prostatic and seminal fluids. In this environment,  $\text{Zn}^{2+}$  is an important component of prostatic fluids, is present at high concentration (4.5 to 7 mM), and has been found to be critical in spermatogenesis [33]. Prostatic secretions are primary components of the antimicrobial defenses of the male genitourinary tract [32].  $\text{Zn}^{2+}$ , in particular, is principal to prostate defense due to its ability to prevent pathogen establishment in the male reproductive tract [33] and has, indeed, been found to have an antimicrobial spectrum towards bacteria, viruses, chlamydiae, and fungi [34]. This antimicrobial effect also affects *T. vaginalis*, which is sensitive to relatively low concentrations of  $\text{Zn}^{2+}$  chloride and sulfate, giving a minimal trichomonocidal concentrations (MTC) of 1.6 mM for both [33]. Nevertheless, a  $\text{Zn}^{2+}$  concentration of about 0.8 mM, obtained in patients with chronic bacterial prostatitis, is not trichomonocidal [35]. In these cases, *T. vaginalis* may persist for longer periods of time in the male genitourinary tract, and possibly progress to the prostate. *T. vaginalis* has been observed to infect the prostatic epithelium, cause chronic prostatitis, and elicit an inflammatory immune response [36]. Thus, *T. vaginalis* has been observed in prostate tissue near inflamed areas and epithelial hyperplasia, which suggests that *T. vaginalis* might be involved in prostate carcinogenesis [37].

Furthermore,  $\text{Zn}^{2+}$  plays an important role in the metabolism of parasites. It interferes in the function of the hydrogenosome, an organelle involved in the metabolism of pyruvate. The hydrogenosome is the main site of the initial  $\text{Zn}^{2+}$  effect in the pathogenic protozoan *Tritrichomonas foetus* [38].

The purpose of the present study was to investigate the morphology of *T. vaginalis* and the proteinases involved in its interaction with DU-145 prostatic cells and to examine the  $\text{Zn}^{2+}$ -dependent changes on the cytotoxicity and protein pro-

file of *T. vaginalis*. The  $\text{Zn}^{2+}$  effect on the protein and transcript levels of TvCP65 and the identification of differentially expressed proteins were of particular interest.

## 2. Material and methods

### 2.1 *T. vaginalis* and cells culture.

Trophozoites of *T. vaginalis* isolate CNCD 147 were axenically cultivated for 24 h in trypticase-yeast extract-maltose (TYM) medium pH 6.2 with 10% heat-inactivated horse serum (Gibco) and supplemented with or without 0.25 mM, 1.0 mM, and 1.6 mM  $\text{ZnCl}_2$  (Sigma). Samples were taken at several time points up to 24 h for parasite counting using a Neubauer-counting chamber, and viability was measured by the trypan blue exclusion method [28]. Cytotoxicity assays and proteomic profiles were performed with parasites cultivated under the same conditions.

Immortalized HeLa ATCC cells were grown in Dulbecco's Modified Eagle's Medium (DMEM; Life Technologies) supplemented with 10% horse serum and 10% penicillin-streptomycin (Gibco) at 37 °C in a 5%  $\text{CO}_2$  atmosphere for 24 h until confluent cell monolayers were obtained. DU-145 ATCC cells were grown in low glucose DMEM (pH 7.2) supplemented with 10% fetal bovine serum and 10% penicillin-streptomycin (Gibco) at 37 °C in a 5%  $\text{CO}_2$  atmosphere for 24 h until confluent cell monolayers were obtained.

### 2.2 2D gel electrophoresis.

For proteomic maps, we used a previously reported protocol [39] with modifications. *T. vaginalis* ( $1.2 \times 10^8$ ) grown in the presence or absence of 0.25 mM, 1.0 mM, and 1.6 mM  $\text{Zn}^{2+}$  were collected by centrifugation at 900 g for 5 min at 4 °C and washed three times with PBS pH 7.0. For the first dimension, parasites were lysed in a final volume of 200  $\mu\text{l}$  rehydration solution (7 M urea, 4% CHAPS, 70 mM DTT, 2% IPG buffer pH 4–7, trace bromophenol blue; Bio-Rad). The supernatant was centrifuged at 13000 g for 10 min at 4 °C to remove insoluble material, and samples of 120  $\mu\text{l}$  (corresponding to  $7.2 \times 10^7$  parasites) were applied to an IPG strip (7 cm, pH 4–7 linear; Bio-Rad) for passive rehydration for 12 h. All isoelectric focusing took place on a Protean IEF system (Bio-Rad) as follows: step 1—gradient from 1 to 225 V over 35 min; step 2—gradient from 250 to 2479 V over 185 min; step 3—gradient from 2466 to 15,434 V over 210 min. Before the second dimension, proteins were reduced (10 mg/ml DTT) and alkylated (25 mg/ml iodoacetamide) step-wise, 15 min for each step, in equilibration buffer (6 M urea, 2% SDS, 300 mM Tris-Cl pH 8.8, 20% glycerol, and 0.002% bromophenol blue) at room temperature. Equilibrated IPG strips were separated on 12% SDS-PAGE gels (7 cm  $\times$  8 cm  $\times$  1.0 mm) using the MiniProtean II Cell vertical system (Bio-Rad) and standard Tris/glycine/SDS buffer. Gels were run at 35 mA/gel at room temperature until the tracking dye left the gel and stained with Coomassie Brilliant Blue G-250 following procedures described by the manufacturer. Finally, gels were documented using Gel Doc EQ (Bio-Rad). Image analysis was performed using the pDQuest software (Bio-Rad). Three

independent protein preparations, each obtained from an independent parasite culture, were performed for comparisons of 2-DE maps. Differentially expressed proteins were determined by a tridimensional analysis using Melanie 7 Software and identified by tandem mass spectrometry analysis (MS/MS).

### 2.3 LC-ESI-MS/MS.

The MS/MS analysis of each fraction obtained from the offline separation steps was carried out on a 3200 Q TRAP hybrid tandem mass spectrometer (Applied Biosystems/MDS Sciex, Concord, ON, Canada) equipped with a nanoelectrospray ion source (NanoSpray II). The instrument was coupled online to a nanoAcquity Ultra Performance LC system (Waters Corporations, Milford, MA). Samples were desalted by injection onto a Symmetry C18 UPLC trapping capillary column (180  $\mu\text{m} \times 20$  mm, Waters Corporations) and washed with 0.1% formic acid in 100% MilliQ water at a flow rate of 15  $\mu\text{l}/\text{min}$ . After 3 min, the trap column was switched in line with a capillary analytical column. Peptides were separated on an ethylene-bridged hybrid, C18 UPL column (75  $\mu\text{m} \times 100$  mm, Waters Corporations) using a linear gradient of 2-70% acetonitrile, 0.1% formic acid over a 60 min period at a flow rate of 0.25  $\mu\text{l}/\text{min}$ . Spectra were acquired in automated mode using Information Dependent Acquisition (IDA). Precursor ions were selected in Q1 using the enhanced MS mode with a scan range of  $m/z$  400-1500 and 4000 amu/s. Selected ions were subjected to an enhanced resolution scan at a low speed of 250 amu/s over a narrow (30 amu) mass range and, then, to an enhanced product ion scan (MS/MS). Precursor ions were fragmented by collision activated dissociation (CAD) in a Q2 collision cell using rolling collision energy. The generated fragment ions were captured and mass analyzed in a Q3 linear ion trap.

### 2.4 Database search.

For protein identifications, the molecular mass of each tryptic fragment was used as query at the National Center for Biotechnology nonredundant database using the MASCOT search algorithm (Matrix Science, London, UK, available at <http://www.matrixscience.com>). Monoisotopic mass values, mass tolerance (peptide  $\pm 1.2$  Da and fragment  $\pm 0.6$  Da), possible methionine residue oxidation, and deamidation and carbamidomethylation at cysteine residues were considered as variable modifications. A maximum of one missed tryptic cleavage per protein was allowed, and no taxonomic restrictions were considered in the database search. For positive identifications, MASCOT individual ion scores  $>56$  indicated identity or extensive homology ( $p < 0.05$ ).

### 2.5 Cell-binding assay.

The cell-binding assay to detect proteinases with affinity to the host cell surface was performed as previously described [15]. Briefly, a clarified detergent extract from  $2 \times 10^7$  parasites, which was grown in the presence or absence of 0.25 mM, 1.0 mM, or 1.6 mM  $\text{Zn}^{2+}$ , was incubated for 18 h at 4 °C with  $1 \times 10^6$  fixed HeLa or DU-145 cells. Then trichomonad

proteinases bound to the surface of fixed cells were eluted in Laemmli buffer [40] for 20 min at 37 °C. Released proteinases were loaded onto a 10% SDS-PAGE gel copolymerized with 2% gelatin and run at 35 mA/gel. Gels were washed with 10% Triton X-100 for 10 min with gentle agitation. Finally, proteinase activation was performed in 100 mM sodium acetate buffer pH 4.5 with 0.1%  $\beta$ -mercaptoethanol for 18 h at 4 °C, 25 °C, 37 °C, and 43.5 °C. The gels were further stained with Coomassie Brilliant Blue for a visualization in which clear bands against a dark background indicate proteolytic activity. Densitometry analyses of activity bands were performed in triplicate using the software Quantity One ver. 4.6.3 (Bio-Rad).

### 2.6 Cytotoxicity assay.

The cytotoxicity assay was carried out using confluent HeLa and DU-145 cells monolayers in 48-well microtiter plates with  $3.5 \times 10^4$  HeLa or  $5.5 \times 10^4$  DU-145 cells/well, respectively. Briefly, parasites ( $2.75 \times 10^5$ ) grown with or without 0.25 mM, 1.0 mM, and 1.6 mM  $\text{Zn}^{2+}$  were resuspended in TYM-DMEM medium without serum, added to confluent cell monolayers of HeLa or DU-145 cells at a ratio of 5:1 (parasites:host cell), and incubated for several time points, up to 24 h, at 37 °C under a 5%  $\text{CO}_2$  atmosphere. Monolayer destruction was assessed using a colorimetric method and quantitated spectrophotometrically at 570 nm [14, 16, 28]. Each sample was performed in triplicate, and experiments were performed at least twice with similar results.

### 2.7 Western blot assay.

Total protein extract from parasites ( $2 \times 10^7$ ), which were grown in the presence or absence of 1.6 mM  $\text{Zn}^{2+}$ , were obtained by TCA-precipitation as previously described [16, 28, 41]. Solubilized proteins were resuspended in Laemmli buffer [40], boiled, and loaded onto a 10% polyacrylamide gel with an equivalent of  $4 \times 10^5$  parasites/lane. Protein extracts were blotted onto nitrocellulose membranes and blocked with 5% skim milk in PBS (pH 7.0) for 18 h at 4 °C. Membranes were incubated for 18 h at 4 °C with anti-TvCP65 primary antibody as reported [16], and an anti- $\alpha$ -tubulin monoclonal antibody (1:1000 dilution, Invitrogen) was used as a loading control. Then the blotted membrane was washed five times with a PBS pH 7.0-0.1% Tween 20 buffer. The primary antibody was detected with a secondary goat anti-mouse-IgG (H+L) horseradish peroxidase conjugate (1:3000 dilution, Invitrogen). The membrane was washed with PBS pH 7.0-0.1% Tween 20 and visualized using an enhanced chemiluminescence ECL Plus Western Blotting Detection System (GE Healthcare) according to the manufacturer's instructions.

### 2.8 RNA extraction and cDNA synthesis.

A sample containing  $2 \times 10^7$  parasites grown with or without 0.25 mM, 1.0 mM, and 1.6 mM of  $\text{Zn}^{2+}$  was collected by centrifugation at 900 g for 5 min at 4 °C (Allegra™ X-22 Centrifuge, Beckman Coulter). The pellet was suspended in 1 ml of TRIzol® reagent (Invitrogen, Life Technologies, Carlsbad,

CA), and the total RNA was extracted as recommended by the manufacturer. RNA concentration was determined spectrophotometrically using a NanoDrop 2000 (Thermo Scientific). All 260/280 ratios were between 1.8 and 2.1. Finally, 1 µg of total RNA was reverse-transcribed using the Superscript Reverse Transcriptase Kit (Invitrogen) and the oligo-dT (dT<sub>18</sub>) (10 pmol/µl) primer.

### 2.9 Analysis of gene expression by semi-quantitative RT-PCR.

PCR was performed in 50 µl reactions containing 50 ng of cDNA, 10 pmol of each primer pair, and 0.25 U of Taq DNA polymerase (Invitrogen). PCR was carried out in a GeneAmp PCR System 9700 thermal cycler (Applied Biosystems). We used the following primer pairs to amplify: 370 bp of the *tvcp65* gene (accession number AY463696), forward: 5'-ACGCGATTACATCTGGAGAACTC-3', and reverse: 5'-ATAAGAGGAGCGTGATGGCACAT-3'; and 112 bp of the *β-tubulin* gene as reported [42]. The amplified products were analyzed on 2% agarose gels and visualized by ethidium bromide staining. Gene expression densitometry analyses were performed using the Quantity One Software (Bio-Rad). Data from densitometry quantification of the housekeeping gene (*β-tubulin*) were used to normalize the results.

### 2.10 Real-time qRT-PCR analysis of specific *T. vaginalis tvcp65* and *β-tubulin* genes.

Quantification of *tvcp65* expression was performed by real-time qRT-PCR. Oligonucleotide primers for real-time qRT-PCR were designed using Primer3 version 3.0 ([www.primer3.sourceforge.net](http://www.primer3.sourceforge.net)) and commercially synthesized (Instituto de Biotecnología, UNAM). To specifically amplify 100 bp of the *tvcp65* gene, the forward: 5'-AATGTTGTTGAAGGCGATGAAA-3', and reverse: 5'-CTACAGCAGCTGGGCCATTT-3' were used, and previously reported primers were used to amplify 112 bp of the *β-tubulin* gene [42]. Each reaction was carried out in a total volume of 25 µl with 1 µl of cDNA (50 ng), 12.5 µl Maxima™ SYBR Green/ROX qPCR Master Mix (2×) kit (Fermentas), 1 µl of each primer (10 pmol/µl), and 9.5 µl of molecular biology grade water. qRT-PCR was performed using a 7500 Fast Real-Time PCR machine (Applied Biosystems). PCR conditions for *tvcp65* were as follows: 15 min at 95°C followed by up to 40 cycles of 95°C for 30 s, 57°C for 30 s, and 72°C for 30 s, and, finally, 95°C for 15 s, 60°C for 30 s, and 95°C for 15 s. The "housekeeping" *β-tubulin* gene was selected for a reference gene study because it did not vary in the presence of any of the tested Zn<sup>2+</sup> concentrations. Standardization of *tvcp65* messenger RNA (mRNA) expression was performed by dividing the value of each gene at different Zn<sup>2+</sup> concentrations by the value of the housekeeping gene found for all sample.

### 2.11 Indirect immunofluorescence assays.

Parasites were fixed using 4% paraformaldehyde for 1 h at 37°C and washed with PBS pH 7.0. Half of the fixed parasites were permeabilized using 1 M HCl for 2 h at room temperature. Parasites were then blocked with 0.2 M glycine for 1 h at

37°C followed by 0.2% fetal bovine serum for 15 min. Then trichomonads were incubated with polyclonal mouse anti-TvCP65 antibody (1:100 dilution) [16] or preimmune sera (PI) for 18 h at 4°C. Next, parasites were incubated with fluorescein isothiocyanate-conjugated anti-mouse immunoglobulins (1:90 dilution, Jackson ImmunoResearch) for 40 min at room temperature. Finally, Vectashield-DAPI mounting solution (Vector Lab) was added, and laser confocal microscopy was performed (Leica, DMLS).

### 2.12 Scanning electron microscopy.

Parasites cultivated in TYM media for 24 h at 37°C were incubated for different periods of time with DU-145 cell monolayers. Glutaraldehyde-fixed samples were dehydrated with increasing concentrations of ethanol, critical-point dried using a Samdri 780 apparatus (Tousimis, Rockville Maryland, USA), coated with gold using a JEOL JFC-1100 ion-sputtering device, and examined using a XL-30 ESEM scanning electron microscope (FEI Company, Eindhoven, The Netherlands).

### 2.13 Statistical analysis.

All data are the means ± standard error of triplicate samples. A statistically significant change between means was determined by ANOVA (*p*) using Sigma Plot 11.0 Software.

## 3. Results

### 3.1 Growth kinetics of *T. vaginalis*.

To investigate the effects of Zn<sup>2+</sup> on *T. vaginalis* development, we first performed growth kinetics in the presence or absence of 0.25 mM, 1.0 mM, and 1.6 mM Zn<sup>2+</sup> (Fig. 1). After

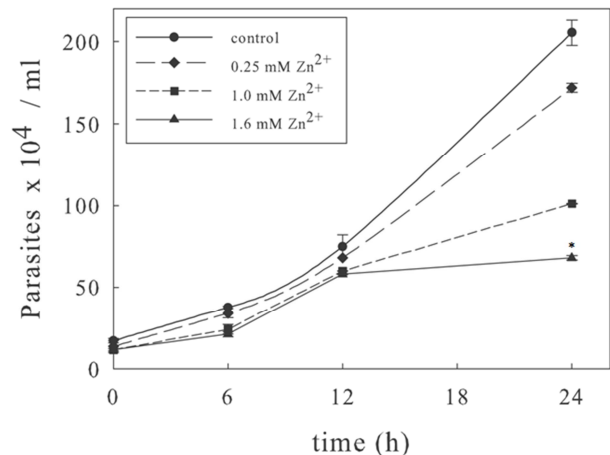


**Figure 1.** Effect of Zn<sup>2+</sup> on the growth of *T. vaginalis*. Parasites were counted in a Neubauer-counting chamber at different time points (6, 12, and 24 h) after incubation at 37 °C in TYM medium supplemented with (0.25 mM, 1.0 mM, and 1.6 mM) or without Zn<sup>2+</sup> (control). In addition, parasite viability, as measured by trypan blue exclusion, was about 98% under all conditions. Each point indicates the mean of three experiments, and error bars indicate standard deviation. There were no statistically significant differences for data corresponding to 0.25 mM (*p*=0.970) and 1.0 mM Zn<sup>2+</sup> (*p*=0.960) compared to the control. In contrast a statistically significant difference was found for 1.6 mM Zn<sup>2+</sup> data (*p*=0.01) (\*) compared to the control.

24 h, the parasites cultivated without  $Zn^{2+}$  (control) had four duplications, while the parasites grown with 0.25 mM, 1.0 mM, or 1.6 mM  $Zn^{2+}$  had three and a half, three, and one duplication, respectively. Furthermore, viability for all samples was ~98%. Experiments were performed in triplicate with the same results. These findings indicate that  $Zn^{2+}$  had no effect on *T. vaginalis* viability, and trichomonad growth was only diminished in 1.6 mM  $Zn^{2+}$ .

### 3.2 *T. vaginalis* $Zn^{2+}$ proteomic map.

Images of three representative 2-DE gels obtained from three independent experiments using parasites grown in the presence and absence of 0.25 mM, 1.0 mM, and 1.6 mM  $Zn^{2+}$  were analyzed by pDQuest software (data not shown), and it was found that most of the protein profile changes were obtained with 1.6 mM  $Zn^{2+}$ . Therefore, we selected this specific concentration for further analyses. The 2-DE protein spot profiles were highly reproducible in terms of both the total number of protein spots and their relative positions and intensities. Coomassie Brilliant Blue G-250 stained gels showed approximately 150 spots in the presence of 1.6 mM  $Zn^{2+}$  (Fig. 2B) compared to 177 spots in its absence (Fig. 2A). Proteins detected in pI 4–7 had molecular masses between 20 and 250 kDa. The gels showed remarkable changes in protein profiles for parasites grown in the presence of  $Zn^{2+}$ . Indeed, we found at least 27 proteins that were differentially expressed in the

presence of  $Zn^{2+}$ . The major differences in expression protein profiles were obtained from 50 to 100 kDa.

Interestingly, we found some spots over-expressed in the presence of  $Zn^{2+}$  (Figs. 2C and 2D, spots 1, 3, 8) that correspond to fimbrin (gi|123493533), adenosylhomocysteinase (gi|123499896), and aminopeptidase P-like metalloproteinase (gi|123445672) (Table 1). Otherwise, the expression levels of several spots were diminished in the presence of  $Zn^{2+}$  (Fig. 2C and 2D). Spots 2, 4, 5, 6, and 7 correspond to fimbrin (gi|123397260) (spots 2 and 4, probably due to degradation), two adenosylhomocysteinases (gi|123499896 and gi|123488577), and asparaginyl endopeptidase-like cysteine peptidase (gi|123408789) (Table 1). These findings suggest that  $Zn^{2+}$  had both positive and negative effects on the expression levels of ~27 proteins and no effect on 111 proteins. Interestingly, the asparaginyl endopeptidase-like cysteine peptidase (gi|123408789) and the adenosylhomocysteinase (gi|123499896) had already been identified in the active degradome of *T. vaginalis* [39].

### 3.3 Proteinases involved in the interaction of *T. vaginalis* and prostatic cells.

We performed ligand-protease assays using parasites grown in the presence or absence of 0.25 mM, 1.0 mM, and 1.6 mM  $Zn^{2+}$  to detect possible *T. vaginalis* proteinases interactions with DU-145 cells. We observed differences between

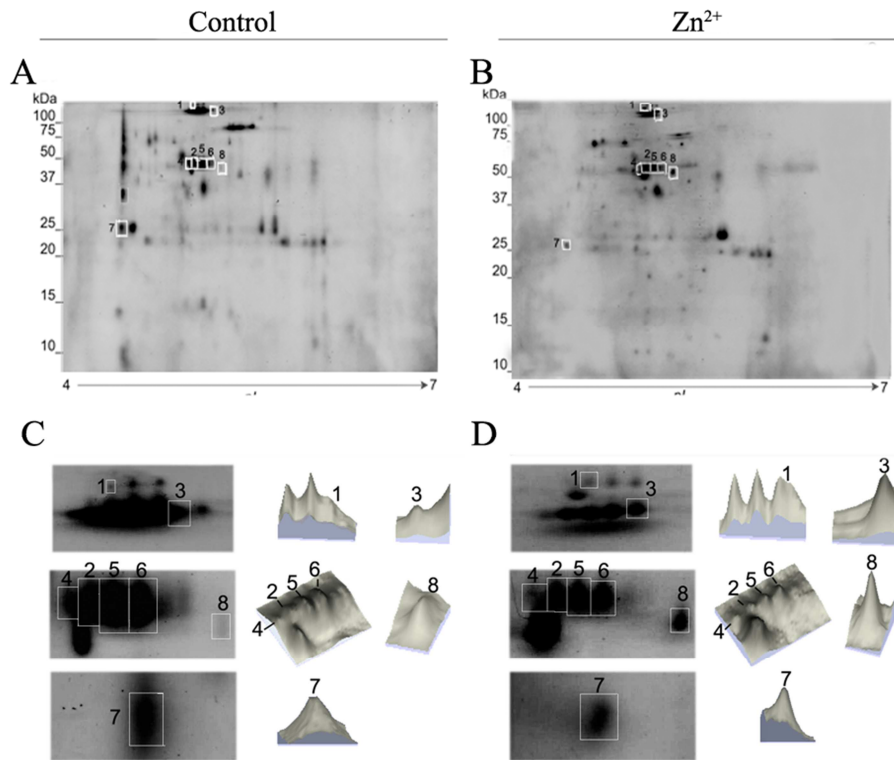


**Figure 2.**  $Zn^{2+}$  proteomic map of *T. vaginalis*. The total proteins of *T. vaginalis* grown in the A) absence or B) presence of 1.6 mM  $Zn^{2+}$  were separated in the first dimension by isoelectric focusing over a pH range from 4.0 to 7.0 followed by 12% SDS-polyacrylamide gel electrophoresis. Protein spots were Coomassie Brilliant Blue G-250 stained. Enlarged images of the gels shown in A or B and three-dimensional analyses of 8 differentially expressed proteins in parasites cultivated in the absence C) or presence D) of  $Zn^{2+}$ . The left panel shows a representative image of a Coomassie Brilliant Blue G-250 gel, whereas the right panel shows a landscape representation of spots. Numbers 1, 3, and 8 indicate spots that are over-expressed in the presence of  $Zn^{2+}$ , while numbers 2, 4, 5, 6, and 7 indicate spots that are down-regulated in the presence of  $Zn^{2+}$ .

the proteinases that interact with DU-145 cells in comparison with those that interact with HeLa cells. [16]. Fig. 3A shows the activities of all proteinases from protein extracts of *T. vaginalis* grown in the absence (Fig. 3A, lane 1) or presence (lane 2) of 1.6 mM Zn<sup>2+</sup>. These extracts interacted with fixed DU-145 cells, and the zymograms show the activities of at least five trichomonad proteinases (TvCP70, TvCP65, TvCP39, TvCP25, and TvCP20) bound to the surfaces of fixed DU-145 cells in the absence (Fig. 3B, lane 1) or presence (lane 2) of 1.6 mM Zn<sup>2+</sup>. Interestingly, the proteolytic activity profile of proteinases that interact with prostatic cells was similar at all temperatures analyzed (data not shown), which suggests that these proteinases may be active up to 43.5 °C. Nevertheless, the best resolution of proteinase activity bands was obtained with activation at 4 °C (Fig. 3B). According to

the densitometry analyses of the TvCP70, TvCP65, TvCP39, TvCP25, and TvCP20 activity bands bound to the DU-145 cells (Fig. 3C), reductions of ~12%, 16%, 13%, 25%, and 11%, respectively, were observed when the parasites were grown in the presence of 1.6 mM Zn<sup>2+</sup> in comparison to the activity bands of untreated control parasites (taken as 100%). Interestingly, the activities of CPs involved in cytotoxicity (TvCP65 and TvCP39) were reduced in the presence of Zn<sup>2+</sup>, however this reduction was minimal. This result may be related to the reduction in trichomonad cytotoxicity observed in the presence of this cation. We also performed Western blot and indirect immunofluorescence assays and real-time PCR experiments to corroborate if the expression levels of these CPs were affected by Zn<sup>2+</sup>.

**Table 1.** Zn<sup>2+</sup> differentially expressed proteins identified by mass spectrometry from clinical isolate *T.vaginalis* CNCD 147 were identified by searching the National Center for Biotechnology non-redundant database using the MASCOT search algorithm.

Protein	Accession number <sup>a</sup>	Spot number <sup>b</sup>	MASCOT score <sup>c</sup>	Ion score <sup>d</sup>	Peptide sequence <sup>e</sup>	% Coverage <sup>f</sup>	Predicted MW Da /pI		
Fimbrin	gi 123493533	1	120	49	K.LSPEQILLR.W	5	67,839 /5.17		
				32	R.LLKPGETLADLLK.L				
				39	K.TVNLTNHPELFR.L				
Fimbrin	gi 123397260	2	125	41	K.LSPEQILLR.W	7	50,761 /6.43		
				43	R.LLKPGETLADLLK.L				
				41	K.TVNLTNHPELFR.L				
				37	R.ALTWPDGK.G				
				37	R.ASDVMIGGK.T				
				58	K.HLDEEVAR.L				
				48	R.HSLIDGINR.A				
				57	K.EMPGLMVLRE				
				22	K.EMPGLMVLRE				
				52	K.SPEGAPFEYR.I				
				49	K.TALVMGYGDVGK.G			30	54,064 /5.61
				23	R.IADINLHVLGR.K				
				55	R.IADINLHVLGR.K				
39	R.LHLGSLDVHLTK.L								
56	K.LLFPAINVNDAVTK.S								
26	K.GFEFENAGAVDPQK.G								
25	K.GDNYEYTCVLAVLK.Q								
43	K.GPQQIVDDGGDATLLIQK.G								
Adenosylhomocysteinase	gi 123499896	4	402	31	K.VYTLPK.H	22	54,064 /5.61		
				44	K.HLDEEVAR.L				
				32	K.SPEGAPFEYR.I				
				69	K.TALVMGYGDVGK.G				
				66	R.IADINLHVLGR.K				
				31	R.LHLGSLDVHLTK.L				
				65	K.LLFPAINVNDAVTK.S				
				27	K.EGTPEKPAGIPVFAWK.G				
				39	K.GPQQIVDDGGDATLLIQK.G				
				36	R.ALTWPDGK.G			33	54,064 /5.61
				53	K.HLDEEVAR.L				
				32	R.HSLIDGINR.A				
				40	K.FDNIYGCR.H				
60	K.SPEGAPFEYR.I								
31	K.TALVMGYGDVGK.G								
59	R.IADINLHVLGR.K								
66	R.IADINLHVLGR.K								
24	R.LHLGSLDVHLTK.L								
54	R.LHLGSLDVHLTK.L								
62	K.LLFPAINVNDAVTK.S								
28	K.QADYINVPVEGPK.S								
45	K.EGTPEKPAGIPVFAWK.G								
39	K.AIVGNIGHFDNEIDTEGLK.N								

				45	R.VIITEVDPICALQAAMEGYQVR.R		
				35	K.VYTLPK.H		
				26	K.KVYTLPK.H		
				45	R.ASDVMIGGK.T		
				39	R.ALTWPDGK.G		
				43	K.HLDEEVAR.L		
				24	R.HSLIDGINR.A		
				47	K.FDNIYGCR.H		
				30	K.EMPGLMVLRE		
				59	K.SPEGAPFEYR.I		
				53	K.TALVMGYGDVGK.G		
	6	850		69	R.IADINLHVLGR.K	48	54,064
				35	K.TALVMGYGDVGK.G		/5.61
				34	R.LHLGSLDVHLTK.L		
				73	K.LLFPAINVNDAVTK.S		
				22	K.QADYINVPVEGPK.S		
				53	K.GFEFENAGAVDPQK.G		
				30	K.GETLPEYWENTYR.A		
				32	K.EGTPEKPAGIPVFAWK.G		
				42	K.GPQQIVDDGGDATLLIQK.G		
				37	K.AIVGNIGHFDNEIDTEGLK.N		
				67	R.VIITEVDPICALQAAMEGYQVR.R		
				44	K.HLDEEVAR.L		
				37	R.HSLIDGINR.A		
				22	K.EMPGLMVLRE		
Adenosylhomocysteinase	gi 1234488577	4	295	34	K.SPAGAPFEYR.I	19	53,873
				60	R.IADINLHVLGR.K		/5.53
				29	R.LHLGSLDVHLTK.L		
				37	K.LLFPAINVNDAVTK.S		
				36	R.VIITEVDPICALQAAMEGYQVR.R		
				42	K.VVAGVPK.L		
				57	K.VTATNFYK.V		
Clan CD, family C13, asparaginyl endopeptidase-like cysteine peptidase	gi 1234408789	7	198	38	R.SLDHLNVYPGR.A	14	43,916
				36	R.SLDHLNVYPGR.		/5.95
				36	K.QSHVMEYGDTSLK.T		
				28	K.IILMCYDDIVNDAENPFK.G		
				61	K.LADEVGGIRI		
				38	K.EVTGVDNVK.F		
				37	R.NVYSILLEK.Q		
Clan MG, family M24, aminopeptidase P-like metallo-peptidase	gi 123445672	8	222	23	K.TPYEIEQIK.K	13	50,416
				31	K.DVYGALDQIK.M		/5.34
				38	K.AAELTSEAIHVMK.N		
				39	K.AAELTSEAIHVMK.N		

<sup>a</sup> NCBI nr database.

<sup>b</sup> Spot number in agreement with Figs. 2A and 2B.

<sup>c,d</sup> Ion score is  $-10 \cdot \log(P)$ , where P is the probability that the observed match is a random event. Individual ion scores > 56 indicate identity or extensive homology ( $p < 0.05$ ). Protein scores are derived from ion scores as a non-probabilistic basis for ranking protein hits.

<sup>e</sup> M = methionine modified by oxidation; N = deamidated; C = cysteine modified by carbamidomethyl.

<sup>f</sup> %Coverage indicates the protein sequences or parts of these sequences that were identified by MS/MS.

Type of search:	MS/MS Ion search
Enzyme:	trypsin
Mass values:	Monoisotopic
Protein Mass:	Unrestricted
Peptide Mass Tolerance:	$\pm 1.2$ Da
Fragment Mass Tolerance:	$\pm 0.6$ Da
Max Missed Cleavages:	1
Instrument type:	ESI-4SECTOR

### 3.4 *T. vaginalis* interaction with DU-145 prostatic cells.

Using scanning electron microscopy, we evaluated the interaction between *T. vaginalis* and DU-145 prostatic cells at several incubation time points (Fig. 4A). The morphology of the parasites in contact with the DU-145 cell monolayer was similar to that of the parasites in contact with HeLa cells. However, their morphology was different in comparison to

those in contact with VEC cells [43]. We observed rounded parasite morphology but never a complete amoeboid transformation during interactions with DU-145 cells (Fig. 4A). After 5 min of incubation, *T. vaginalis* showed adherence to DU-145 cells (Fig. 4A, b). Parasites displayed an oval form with a rough surface, four anterior flagella, an undulating membrane, and posterior axostyle. At the 15 and 30 min time

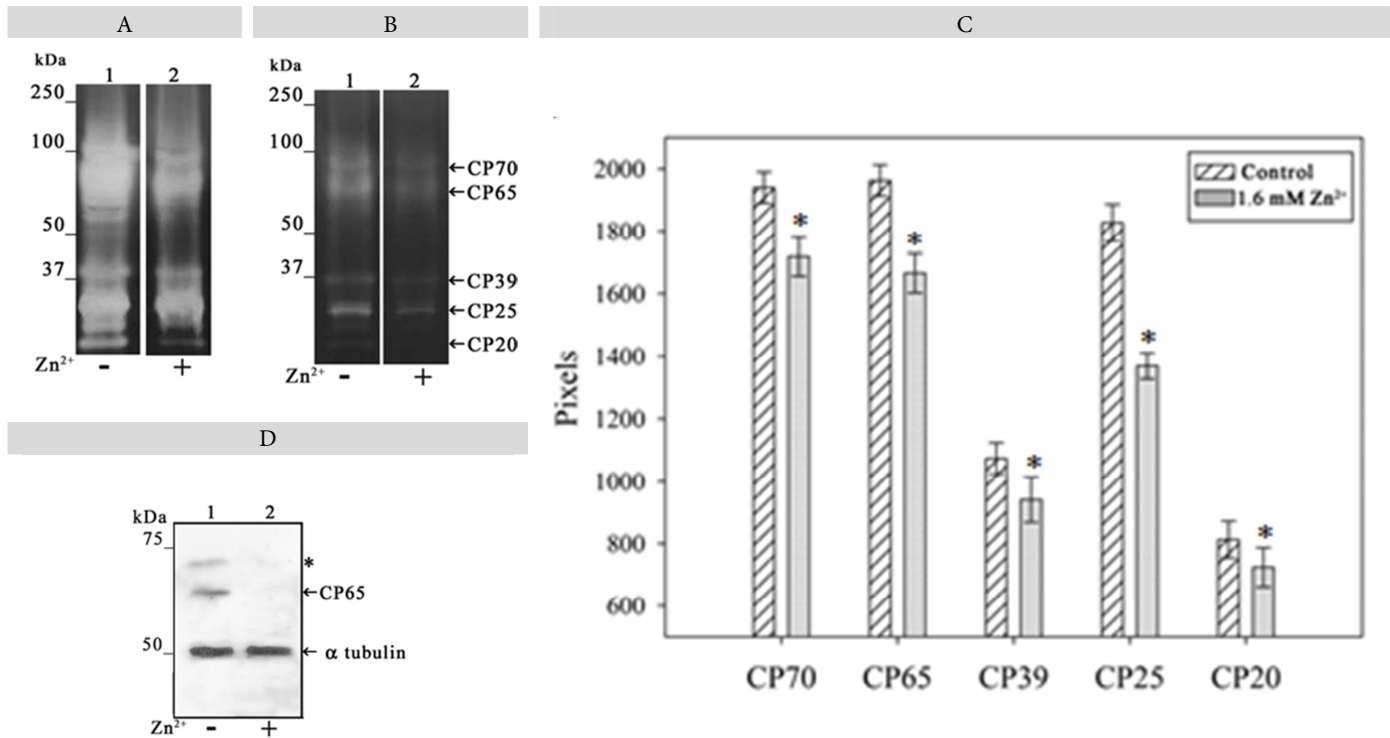


**Figure 3.** Proteinases involved in the interaction of *T. vaginalis* with prostatic cells. A) Zymograms correspond to trichomonad lysates from parasites cultivated in the absence (lane 1) or presence of 1.6 mM Zn<sup>2+</sup> (lane 2). B) Lysates from parasites cultivated in the presence or absence of Zn<sup>2+</sup> were used for ligand-proteinase assays and activated at 4 °C as described in the Materials and Methods section. Proteinase patterns correspond to the trichomonad proteinases with affinity for DU-145 cell surface from parasites cultivated in the absence (lane 1) or presence of 1.6 mM Zn<sup>2+</sup> (lane 2). Arrows show clear bands of the proteolytic activities of 70, 65, 39, 25 and 20 kDa (TvCP70, TvCP65, TvCP39, TvCP25, and TvCP20), respectively. C) Densitometry analyses of each activity band from three different gels activated at 4 °C. Bars indicate the mean intensity of activity bands, and error bars represent the standard deviations *p*=0.01 (\*). D) The Zn<sup>2+</sup> effect on the amount of TvCP65 and  $\alpha$ - tubulin. Total protein extracts from *T. vaginalis* grown in the absence (lane 1) or presence of Zn<sup>2+</sup> (lane 2) were blotted onto nitrocellulose membranes for a Western blot assay with anti-TvCP65 and anti- $\alpha$ -tubulin (control) antibodies. Arrow indicates the immunodetected protein for each antibody employed. Asterisk indicates a higher sized band also recognized by the anti-TvCP65 antibody that might correspond to immunodetection of the TvCP65 precursor band.

points, we observed parasites in close proximities to the same target cells (Fig. 4A, c-d), which was probably due to a chemotaxis effect. After 60 min, we further observed empty areas that became progressively larger after 90 min, which corresponded to monolayer disruptions (Fig. 4A, e). After 90 min, we observed *T. vaginalis* pseudopods forming at the contact site (Fig. 4A, f). Interestingly, amoeboid trophozoites were not observed in contact with DU-145, however amoeboid trophozoites have been observed in contact with VECs [43]. In addition, the integrity and appearance of DU-145 prostatic cells without trichomonads did not change (Fig. 4A, a). We then kinetically analyzed the cytotoxicity of *T. vaginalis* towards DU-145 cells at several different time points (Fig. 4B). With scanning electron microscopy, we observed *T. vaginalis* attached to DU-145 cells after 5 min of incubation (Fig. 4B, b). After 15 min, the monolayer of DU-145 cells began to suffer damage, which might have been due to contact-dependent mechanisms (Fig. 4B, c). After 30 and 60 min, we observed irreversible cell damage due to the trichomonads (Fig. 4B, d, e). The no trichomonad control showed no changes in the appearance of DU-145 cells (Fig. 4B, a).

### 3.5 Cytotoxicity.

First, we determined the Zn<sup>2+</sup> effect on trichomonad cytotoxicity towards HeLa or DU-145 cells. After 1 h, the cytotoxicity exhibited by parasites, which were cultivated with 1.6 mM Zn<sup>2+</sup>, towards HeLa cells was 98% of that exhibited by parasites cultivated in absence of Zn<sup>2+</sup> (Fig. 5A). However, trichomonad cytotoxicity towards DU-145 cells was only 20% of what was seen with HeLa cells, and the presence or absence of Zn<sup>2+</sup> had no effect (Fig. 5A). These findings suggested that Zn<sup>2+</sup> had no effect on *T. vaginalis* cytotoxicity towards HeLa cells; however, trichomonad cytotoxicity towards DU-145 cells at this same time point was 80% less in comparison to HeLa cells (Fig. 5A). We then determined the cytotoxicity of *T. vaginalis* towards prostatic DU-145 cells at different time points and found 100% cytotoxicity after 8 h (Fig. 5B), which suggested trichomonad cytotoxicity was different for HeLa compared to DU-145 cells. In addition, we analyzed the effects of 0.25 mM, 1.0 mM, and 1.6 mM Zn<sup>2+</sup> on the cytotoxicity of DU-145 cells and found that major cytotoxic differences were obtained with 1.6 mM Zn<sup>2+</sup> (data not shown). The kinetic data show that cytotoxicity was 20% at 1

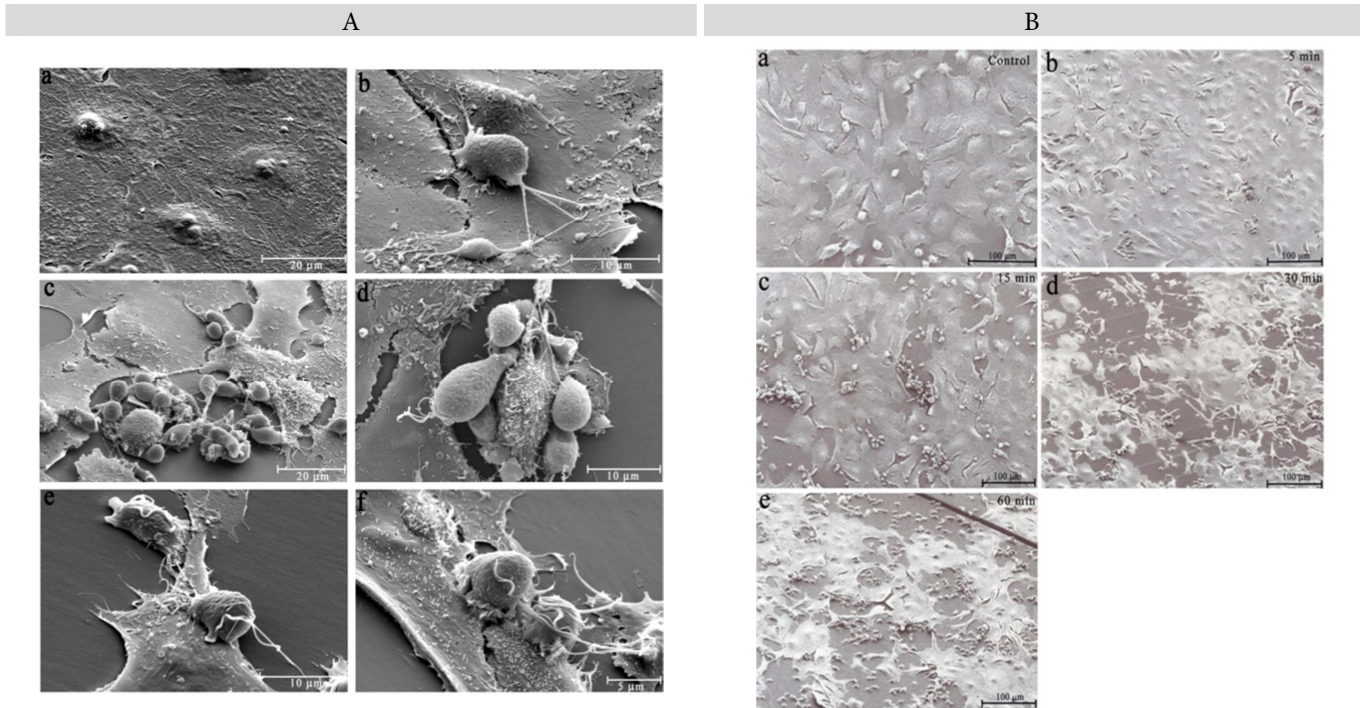


**Figure 4.** Interaction of *T. vaginalis* trophozoites with DU-145 prostatic cell monolayers. Morphological appearance of *T. vaginalis* in contact with DU-145 prostatic cells at different time points, and kinetic studies of the cytotoxicity of *T. vaginalis* towards DU-145 cells. A) Trophozoites were incubated with DU-145 cells for b) 5 min, c) 15 min, d) 30 min, e) 60 min, and f) 90 min. a) DU-145 prostatic cells before interacting with *T. vaginalis*. The majority of parasites attached to DU-145 cells retain a pear-like shape with four flagella, an undulating membrane, and axostyle. Some showed a few pseudopods (panel d-e). After 5 min of interaction, the lytic activity of the parasites is evident as seen by the disruption of the cell monolayer. B) Kinetics of *T. vaginalis* cytotoxicity towards DU-145 cell monolayers. Parasites were added to confluent DU-145 cell monolayers and observed under low magnification by scanning electron microscopy at different time points. Cells show a similar lytic activity at b) 5 min, c) 15 min, d) 30 min, and e) 60 min, as previously described. a) Control DU-145 cells without parasites.

h for parasites cultivated with or without 1.6 mM of  $Zn^{2+}$  (Fig. 5B). After 8 h, the cytotoxicity of parasites cultivated with 1.6 mM of  $Zn^{2+}$  was 72% (Fig. 5B), while in the absence of  $Zn^{2+}$  the cytotoxicity was 100%. These findings suggested that  $Zn^{2+}$  had some negative effect on trichomonal cytotoxicity towards DU-145 cells.

### 3.6 The effect of $Zn^{2+}$ on the amount of TvCP65.

By Western blot analysis, an anti-TvCP65 antibody [16] immunodetected two bands that correspond to a precursor (Fig. 3D, lane 1 asterisk) and active TvCP65 enzyme (Fig. 3D, lane 1 arrow) in total protein extracts from parasites grown without  $Zn^{2+}$ . In contrast, parasites grown in the presence of  $Zn^{2+}$  lacked these bands (Fig. 3D, lane 2), while an anti- $\alpha$ -tubulin antibody detected a single band with the same intensity in the absence (Fig. 3D, lane 1) or the presence of  $Zn^{2+}$  (lane 2). As expected, the amount of  $\alpha$ -tubulin was not changed in the presence of  $Zn^{2+}$ , which indicated the  $Zn^{2+}$  effect was specific for the TvCP65 protein level. These observations suggest that the amount of TvCP65 was reduced in the presence of  $Zn^{2+}$ , which could be related to the reduction in the cytotoxicity level.

To confirm the decrease in TvCP65 protein level in *T. vaginalis*, indirect immunofluorescence assays were performed using permeabilized and non-permeabilized fixed parasites. Fig. 6 shows a reduction of fluorescence intensity

from surface (panels k and l) and cytoplasmic (panels h and i) TvCP65 in  $Zn^{2+}$ -treated trichomonads compared to the control trichomonads, which show fluorescence on the surface (panels e and f) and in the cytoplasm (panels b and c). No fluorescence was observed from trichomonads treated identically but incubated with PI serum, a negative control (panels n and o). These data strongly suggested that the presence of  $Zn^{2+}$  affects the amount of TvCP65, which resulted in a reduction in the TvCP65 proteolytic activity.

### 3.7 The effect of $Zn^{2+}$ on tvcp65 mRNA.

We then performed semi-quantitative and quantitative RT-PCR (Fig. 7) using cDNA from parasites grown in the presence or absence of  $Zn^{2+}$  to determine the effect of  $Zn^{2+}$  on the expression of the TvCP65 transcript. We obtained a 370-bp amplicon using cDNA from parasites grown in the absence (Fig. 7A, lane 1) or presence of 1.6 mM  $Zn^{2+}$  (lane 2). Based on densitometry analyses (data not shown), an 80% reduction, compared to the no  $Zn^{2+}$  control, was observed for tvcp65 transcript. The 112-bp  $\beta$ -tubulin RT-PCR product was used as an internal control. As expected, the quantity of this transcript was not affected by the  $Zn^{2+}$  concentration (Fig. 7B, lanes 1-2). No detectable PCR product from DNaseI-treated RNA from parasites cultivated in the presence or absence of  $Zn^{2+}$  was obtained in the negative controls (RT(-) experiments)(Figs. 7A and 7B, lanes 3-4), which showed that ampli-

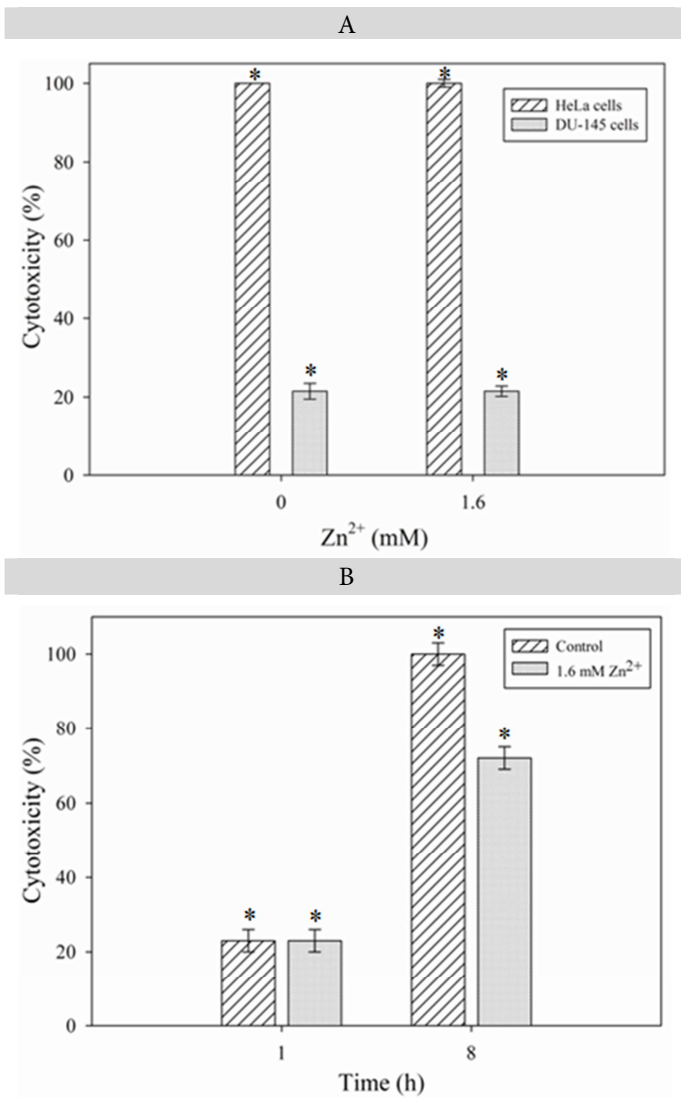


**Figure 5.** Zn<sup>2+</sup> effect on *T. vaginalis* cytotoxicity. Kinetic cytotoxicity of parasites cultivated in the presence or absence of 1.6 mM Zn<sup>2+</sup>. A) Cytotoxicity of *T. vaginalis* cultivated in the presence and absence of Zn<sup>2+</sup> towards HeLa and DU-145 cells after 1 h,  $p=0.056$  (\*). B) Data from trichomonal cytotoxicity towards DU-145 cells after 8 h without Zn<sup>2+</sup> were normalized to 100% for comparison. Cytotoxicity of *T. vaginalis* cultivated with 1.6 mM Zn<sup>2+</sup> was reduced 30%. Bars indicate the percent cytotoxicity of three experiments with triplicate samples, and error bars represent standard deviations,  $p=0.050$  (\*).

cons from *tvcp65* and  $\beta$ -*tubulin* genes corresponded to the quantity of mRNA of each gene. Consistent with these findings, the qRT-PCR results indicated that the *tvcp65* transcript was reduced 80% in the presence of Zn<sup>2+</sup> (Fig. 7C).

#### 4. Discussion

Zn<sup>2+</sup> is a catalytic component of over 300 enzymes [44]. This metal is an essential nutrient and plays a crucial role in several biological functions in the male microenvironment. Zn<sup>2+</sup> is a part of several proteins as both a structural and catalytic component, such as DNA-binding proteins, which contain Zn<sup>2+</sup> fingers, and the CCCH-type Zn<sup>2+</sup> finger protein, which participates in the adenylation and export of metazoan nuclear mRNAs [45]. Moreover, Zn<sup>2+</sup> has many functions in

proteins, which include metalloregulation and Zn<sup>2+</sup> signaling [46]. Human prostatic fluid from healthy men and men with chronic bacterial prostatitis or trichomoniasis has different Zn<sup>2+</sup> concentrations [34]. Indeed, Zn<sup>2+</sup> levels found in the prostate could be important in resolving trichomoniasis in men [29, 34].

Our results with human DU-145 prostatic cells showed morphological and molecular changes of *T. vaginalis* that might contribute to understanding how this parasite causes damage to men. We analyzed different Zn<sup>2+</sup> concentrations and found that the major differences in cytotoxicity, duplication, and protein profile were obtained at 1.6 mM Zn<sup>2+</sup>, which is the minimum trichomonicidal concentration (MTC) [34] for *T. vaginalis*. In fact, survival of parasites in the presence of Zn<sup>2+</sup> was proportional to the Zn<sup>2+</sup> concentration. Nevertheless, parasite viability was not affected by Zn<sup>2+</sup>. As pointed out by Krieger and Rein, normal human prostatic fluid Zn<sup>2+</sup> concentrations kill *T. vaginalis in vitro* and may limit or solve trichomoniasis in most infected men [34]. Studies indicate that *T. vaginalis* survival in canine prostatic fluid is not significantly different from survival in Zn<sup>2+</sup> with a similar cation concentration [34]. This is not the case for *Tritrichomonas foetus*, which is unaffected by bovine seminal fluid. *T. foetus*

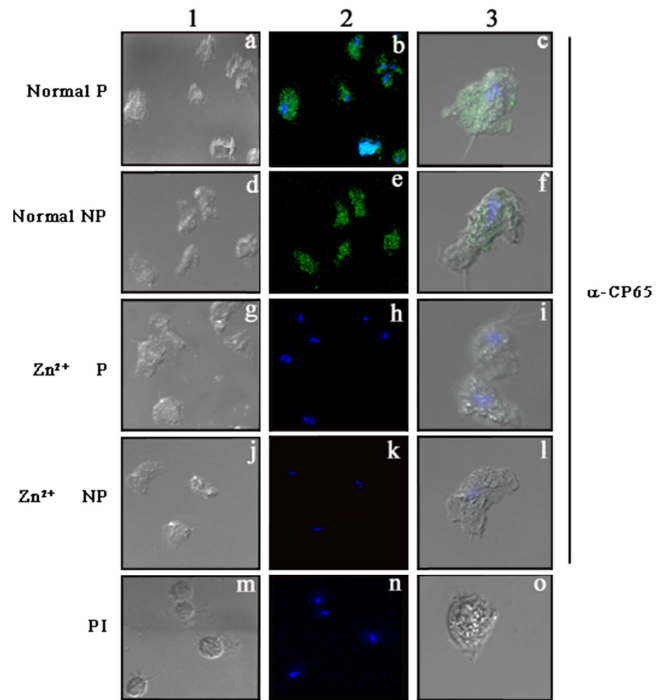


**Figure 6.** Expression and localization of TvCP65 in the presence of Zn<sup>2+</sup>. Immunofluorescence analyses of fixed, non-permeabilized (NP; d-f, j-l) and permeabilized (P; a-c, g-i) parasites grown in the presence (g-l) or absence (a-f, m-o) of 1.6 mM Zn<sup>2+</sup>, incubated with the anti-TvCP65 antibody (a-l) or preimmune sera (PI; m-o) followed by a secondary anti-mouse conjugated to a fluorescein isothiocyanate (Jackson) antibody (1:90 dilution), and mounted with Vectashield-DAPI. Indirect immunofluorescence (b, e, h, k), and the corresponding phase contrast microscopy at 60 $\times$  magnification (a, d, g, j) and 1.58 zoom (c, f, i, l). As a negative control, permeabilized parasites were incubated with PI (m-o) at a 1:20 dilution.

has an MTC of 200 mM for  $Zn^{2+}$ , which is far higher than the  $Zn^{2+}$  concentration found in the reproductive tract of a bull [29].

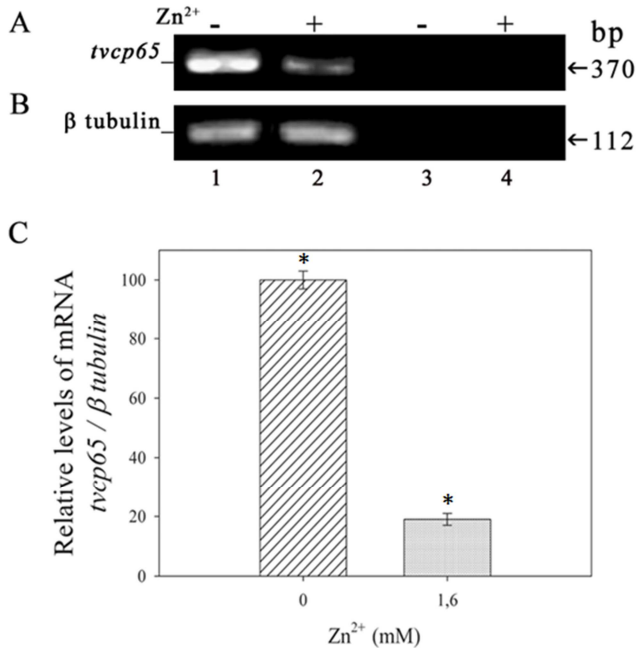


**Figure 7.**  $Zn^{2+}$  effect on the expression level of *T. vaginalis tvcp65* mRNA. Semi-quantitative RT-PCR analyses to detect the A) 370-bp *tvcp65* or B) 112-bp  $\beta$  tubulin transcript using cDNA from parasites cultivated in the absence (lanes 1) or presence 1.6 mM (lanes 2) of  $Zn^{2+}$  and RT(-) a negative control from parasites cultivated in the absence (lanes 3) or presence of 1.6 mM  $Zn^{2+}$  (lanes 4). Arrows indicate the 370-bp and 112-bp RT-PCR products for the *tvcp65* and  $\beta$ -tubulin transcripts, respectively. These experiments were performed at least three times with similar results. C) qRT-PCR to quantify levels of *tvcp65* mRNA in trichomonads using cDNA from parasites cultivated in the absence or presence of 1.6 mM  $Zn^{2+}$ . Data were normalized to the amount of  $\beta$ -tubulin mRNA (quantity of *tvcp65* mRNA/quantity of  $\beta$ -tubulin mRNA). Bars show means of relative amounts of RT-PCR products from three separate experiments, and errors bars indicate standard deviation,  $p=0.01$  (\*).

Evidence indicates that *T. vaginalis* is not the only human parasite affected by  $Zn^{2+}$  levels. *Entamoeba histolytica* replication and adhesion is decreased in the presence of  $Zn^{2+}$ , which results in an inhibition of amoebic pathogenicity *in vivo* [47]. The activities of amoebic CPs are specifically inhibited by this cation. Interestingly, this  $Zn^{2+}$  inhibitory effect is reversible [48]. In men, prostate  $Zn^{2+}$  levels might inhibit the activities of *T. vaginalis* CPs, which may affect its cytotoxicity. This could be one of the reasons why male trichomoniasis is less severe.

When *T. vaginalis* attaches to VECs, it undergoes a rapid transformation to an amoeboid morphology [9]. Nevertheless, the parasites were not transformed when they came into contact with DU-145 prostatic cells. Furthermore, we observed extensive membrane interdigitations between parasite membranes and prostatic cells. This behavior has also been observed in parasites in contact with VECs [9]. There is a possibility that trichomonads that undergo morphological

transformations to amoeboid forms might have enhanced virulence capabilities [9]. Thus, the *T. vaginalis* amoeboid transformation did not occur with DU-145 prostatic cells, which resulted in lower cytotoxicity levels in those cells. This observation agrees with the diminished cytotoxicity levels of parasites grown in a similar prostate microenvironment due to the presence of  $Zn^{2+}$ . In addition, certain components of the vaginal microenvironment, such as  $Fe^{2+}$ , also influence the morphology of *T. vaginalis*.  $Fe^{2+}$  depletion induces morphological changes in this parasite from ellipsoid or amoeboid trophozoites to rounded ones, which is followed by flagella internalization and axostyle invagination [49], a pseudocyst morphology.

In addition,  $Zn^{2+}$  also affects the protein profile of *T. vaginalis*. Some proteins were up- or down-regulated in the presence of  $Zn^{2+}$ , while others showed no changes. A similar behavior was observed in the proteome of *T. vaginalis* in the presence or absence of  $Fe^{2+}$  [49], which is crucial in the female microenvironment and produces changes in its proteome. Forty-five proteins were found to be differentially expressed [49]. Because *T. vaginalis* is able to infect men, it can possibly adapt to the prostate microenvironment, survive, and establish an infection. We have demonstrated that *T. vaginalis* differentially expresses 27 proteins in the presence of  $Zn^{2+}$ , which suggests this parasite has the capability to adapt to different environments. These differences in protein expression profiles correlated with changes in some of its virulence properties, such as cytotoxicity.

We found that fimbrin (gi|123493533) and the aminopeptidase P-like metalloproteinase from Clan MG, family M24 (gi|123445672) were over-expressed in the presence of  $Zn^{2+}$ . In contrast, another fimbrin (gi|123397260), the asparaginyl endopeptidase-like cysteine peptidase (gi|123408789), and a different isoform of adenosylhomocysteinase (gi|123499896) were down-expressed with  $Zn^{2+}$ .

Fimbrins belong to a class of actin-bundling proteins that are components of the actin cytoskeleton and involved in many biological phenomena [50]. As an example, mutant *Saccharomyces cerevisiae* lacking the fimbrin gene display temperature sensitivity defects in growth, morphology, endocytosis, and sporulation [51-52]. However, over-expression of this protein is lethal [53]. In the male microenvironment, *T. vaginalis* faces a high  $Zn^{2+}$  concentration that induces the over-expression of fimbrin. This may be related to the morphological appearance of the parasite in the male microenvironment. In contrast, another fimbrin is down-regulated in the presence of this cation. Further studies are in progress to determinate the role of these two fimbrins in the biology of *T. vaginalis*.

Only two metalloproteinases (142 and 220 kDa) from *T. vaginalis* grown under normal culture conditions have been described [54]. This is the first report of a 50 kDa metalloproteinase from *T. vaginalis* expressed in the presence of  $Zn^{2+}$ . Moreover, *T. vaginalis* proteases are involved in many biological functions, including virulence, as virulence factors [16-17], participating in hemolysis [21], complement resistance

[22], cytotoxicity [18-19], apoptosis induction [24], nutrient acquisition [21, 55], and immune evasion [22-23]. It is possible that in the presence of  $Zn^{2+}$  *T. vaginalis* expresses this metalloproteinase for survival and colonization of the male microenvironment. We are in the process of purifying and characterizing this enzyme and determining its cellular localization and function.

Our findings indicate that it takes the parasite more time to cause damage to the prostatic DU-145 cell monolayers as compared to HeLa cell monolayers. This may be due to different cellular receptors. *T. vaginalis* presents a specific behavior according to its host. For example, although trichomonad adherence to HeLa and VEC cells occurs through the same adhesins [12], only VECs are capable of signaling for amoeboid transformation [9]. In addition, the density of particular receptors might also be involved in the responses from the parasite to different cell types.

Trichomonal cytotoxicity towards cervical cells includes the activity of different molecules, including proteinases. Its expression is induced under iron-depleted conditions [16, 18-19, 28], which increase trichomonal cytotoxicity levels towards HeLa cell monolayer due to an increase in TvCP65 proteolytic activity [28].  $Zn^{2+}$  particularly negatively affects the cytotoxicity of *T. vaginalis* towards DU-145 cells. Our results suggest that five *T. vaginalis* CPs (TvCP70, TvCP65, TvCP39, TvCP25, and TvCP20) were involved in contacting prostatic cells, and their proteolytic activities were negatively affected by  $Zn^{2+}$ . Interestingly, the CPs involved in cytotoxicity (TvCP65 and TvCP39) [16, 18-19, 28] also interacted with DU-145 cells, and their activities were negatively affected by  $Zn^{2+}$ . These findings might explain the reduction in cytotoxicity levels towards prostatic cells in the presence of  $Zn^{2+}$ , i.e., because of its inhibitory effect towards the CPs involved in cellular damage. Furthermore,  $Zn^{2+}$  inhibits a great number of proteins and functions, including CPs, signaling by phosphorylation, mitochondrial respiration, and neurotransmission. All of these are examples of the biological importance of  $Zn^{2+}$  inhibition [56].

One of the CPs involved in the *T. vaginalis* interaction with prostatic cells is TvCP65. It has previously been reported that TvCP65, which is located on the plasma membrane and in cytoplasm, has an important role in trichomonal cellular damage towards HeLa cell monolayers [16]. However, in the presence of  $Zn^{2+}$ , this molecule was not observed by immunofluorescence assays. The activity, protein level, and transcript of TvCP65 were negatively affected by  $Zn^{2+}$ , which led to a reduction in TvCP65-dependent cytotoxicity. TvCP65 proteolytic activity depends on the pH and the substrate. TvCP65 degrades collagen IV and human fibronectin at pH 3.6-7.5 and 3.6-6.0, respectively [16]. During *T. vaginalis* infections, the prostate pH changes. At the beginning of a male infection, the pH is about 7.0-7.5. When the infection is already established, the microenvironment pH changes to 8.0-8.5 [57]. Thus, TvCP65 might be implicated in prostatic cell damage at the beginning of the infection due to its activity at that pH range [16]. pH variations during male infections

might affect the activity of proteinases such as TvCP65 involved in the interaction of trichomonads and prostatic cells. TvCP65 degrades many substrates and interacts with DU-145 cells, this proteinase might bind to a specific receptor on the prostatic cell surface and be involved in nutrient acquisition mechanisms from different sources found in the male microenvironment.

According to the qRT-PCR results, the *tvcp65* mRNA level diminished in the presence of 1.6 mM  $Zn^{2+}$ . Although the proteolytic activity and amount of TvCP65 and its transcript diminished by 80% in the presence of  $Zn^{2+}$ , its cytotoxicity only decreased by 30%. It is important to mention that trichomonal cytotoxicity is a multifactorial process that includes the activity of porins for pore formation [58], contact-dependent disruption of the host cell membrane cytoskeleton [59], a cell-detaching factor [60], and the TvCP39 proteolytic activity [18-19], which might aid in trichomonal cytotoxicity in the presence of  $Zn^{2+}$ . We are in the process of determining the effect of  $Zn^{2+}$  on the amount of protein and transcript of TvCP39 to solve this question. Nevertheless, the possible mechanism of  $Zn^{2+}$  regulation is still unknown. However, it is known that several motifs found in transcriptional regulatory proteins are stabilized by  $Zn^{2+}$ , including the  $Zn^{2+}$  finger,  $Zn^{2+}$  clusters, RING finger, and LIM domains, and proteins that contain these domains are very common [44]. Evidence indicates that  $Zn^{2+}$  sensing in eukaryotes involves occupancy of the  $Zn^{2+}$  finger domains and their interactions with DNA [44]. The metal response element (MRE)-binding transcription factor-1 senses cellular  $Zn^{2+}$  ion concentrations in multicellular eukaryotes and activates the expression of proteins involved in the mechanisms of  $Zn^{2+}$  homeostasis. These types of sensors have been reported in *S. cerevisiae* and termed the  $Zn^{2+}$  responsive activator protein 1 (ZAP1), which has seven  $Zn^{2+}$  finger motifs [46]. Target genes regulated by ZAP1 include the  $Zn^{2+}$  transporter genes (*ZRT1* and *ZRT2*) and the *ZAP1* gene itself [46]. Authors have proposed that *ZAP1* encodes a transcriptional activator that binds to the promoters of these genes and activates their transcription when intracellular  $Zn^{2+}$  levels are low [46]. A similar  $Zn^{2+}$  sensing mechanism might be present in *T. vaginalis* that could result in different profile protein expressions in the presence of  $Zn^{2+}$ . However, there is no experimental evidence that *T. vaginalis* has a  $Zn^{2+}$  transcriptional activator or repressor. Nevertheless, a post-transcriptional regulatory mechanism mediated by an IRE/IRP-like system for TvCP4, a proteinase from *T. vaginalis*, has recently been described [61]. This post-transcriptional mechanism of  $Fe^{2+}$  regulation is based on the interactions of cytoplasmic  $Fe^{2+}$  regulatory proteins (IRPs) with  $Fe^{2+}$ -responsive elements (IREs) located in the untranslated regions (UTRs) of mRNAs of  $Fe^{2+}$ -regulated proteins [62]. A similar mechanism might regulate *tvcp65* mRNA in the presence of  $Zn^{2+}$ . Further studies are needed to solve this question.

## 5. Conclusions

Our results suggest that  $Zn^{2+}$  negatively affects growth, cy-

toxicity, and the expression of *T. vaginalis* proteinases related to the interaction with prostatic cells, which include those involved in trichomonal cytotoxicity, such as TvCP65. This is the first report of a 50 kDa metalloproteinase from *T. vaginalis* expressed in the presence of Zn<sup>2+</sup>. Further studies are necessary to elucidate the mechanism of *T. vaginalis* Zn<sup>2+</sup> regulation.

### Acknowledgements

The authors thank the Posgrado en Ciencias Genómicas at Universidad Autónoma de la Ciudad de Mexico (UACM) and CINVESTAV-I.P.N. We thank UACM for a scholarship to LIVC. LIQG was supported by a scholarship from CONACyT, Mexico. BICG was supported by a scholarship from ICyTDF, Mexico We thank M.Sc Eduardo Carrillo for technical assistance and Javier Mora for proofreading this manuscript. This work was supported by ICyTDF (PIFUTP08-150) and CONACyT (83808) to EAS.

### References

- Arroyo, R. and Alderete, J.F., *Infect. Immun.*, (1989)57: p. 2991-2997.
- Guenther, P.C., Secor, W.E., and Dezzutti, C.S., *Infect. Immun.*, (2005)73: p. 4155-4160.
- El-Shazly, A.M., et al., *J Egypt Soc Parasitol.*, (2001)31: p. 545-553.
- Cotch, M.F., et al., *Sex. Transm. Dis.*, (1997)24: p. 353-360.
- Viikki, M., et al., *Acta Oncol.*, (2000)9: p. 71-75.
- Schwebke, J.R. and Burgess, D., *Clin. Microbiol. Rev.*, (2004)17: p. 794-803.
- Alderete, J.F. and Garza, G.E., *Infect. Immun.*, (1985)50: p. 701-708.
- Alderete, J.F., et al., *Infect. Immun.*, (1988)56: p. 2558-2562.
- Arroyo, R., et al., *Mol. Microbiol.*, (1993)7: p. 299-309.
- Moreno-Brito, V., et al., *Cellular Microbiology*, (2005)7: p. 245-258.
- Garcia, A.F., et al., *Molecular Microbiology*, (2003)47: p. 1207-1224.
- Arroyo, R., Engbring, J., and Alderete, J.F., *Mol. Microbiol.*, (1992)6: p. 853-862.
- Hernández, H., et al., *Parasite Immunol.*, (2004)26: p. 119-125.
- Mendoza-Lopez, M.R., et al., *Infect. Immun.*, (2000)68: p. 4907-4912.
- Arroyo, R. and Alderete, J.F., *Arch. Med. Res.*, (1995)26: p. 279-285.
- Alvarez-Sanchez, M.E., et al., *Microbial Pathogenesis*, (2000)28: p. 193-202.
- Solano-González, E., et al., *International J. of Biochem. and Cell Biol.*, (2006)38: p. 2114-2127.
- Hernández-Gutiérrez, R., et al., *Exp. Parasitol.*, (2004)107: p. 125-135.
- Hernandez-Gutierrez, R., Ortega-López, J., and Arroyo, R., *J. Euk. Microbiol.*, (2003)50: p. 696-698.
- Rendon-Maldonado, J.G., et al., *Exp. Parasitol.*, (1998)89: p. 241-251.
- Dailey, D.C., Chang, T.H., and Alderete, J.F., *Parasitol.*, (1990)101: p. 171-175.
- Alderete, J.F., Provenzano, D., and Lehker, M.W., *Microb. Pathog.*, (1995)19: p. 93-103.
- Provenzano, D. and Alderete, J.F., *Infect. Immun.*, (1995)63: p. 3388-3395.
- Sommer, U., et al., *J. Biol. Chem.*, (2005)280: p. 23853-23860.
- Gorrell, T.E., *J. Bacteriol.*, (1985)161: p. 1228-1230.
- Lehker, M.W., Arroyo, R., and Alderete, J.F., *J Exp Med*, (1991)174: p. 311-318.
- Alderete, J.F., *Infect. Immun.*, (1999)67: p. 4298-4302.
- Alvarez-Sánchez, M.E., et al., *Microbes and Infection*, (2007)9: p. 1597-1605.
- Langley, J.G., Goldsmid, J.M., and Davies, N., *Genitourin Med.*, (1987)63: p. 264-267.
- Krieger, J.N., *Invest Urol.*, (1981)18: p. 411-417.
- Benchimol, M., et al., *Parasitol. Res.*, (2008)102: p. 597-604.
- Krieger, J.N., *Sex. Transm. Dis.*, (1995)22: p. 83-96.
- Krieger, J.N. and Rein, M.F., *J. Infect. Dis.*, (1982)146: p. 341-345.
- Krieger, J.N. and Rein, M.F., *Infect. Immun.*, (1982)37: p. 77-81.
- Fair, W.R., Couch, J., and Wehner, N., *Urology*, (1976)7: p. 169-177.
- Gardner, W.A.J., Culberson, D.E., and Bennet, B.D., *Arch. Pathol. Lab. Med.*, (1986)110: p. 430-432.
- Sutcliffe, S., et al., *International J. Cancer*, (2009)124: p. 2082-2087.
- Benchimol, M., et al., *Antimicrob. Agents Chemother.*, (1993)37: p. 2722-2726.
- Ramon-Luing, L.A., et al., *Proteomics*, (2010)10: p. 435-444.
- Laemmli, U.K., *Nature*, (1970)227: p. 680-685.
- Carvajal-Gamez, B., et al., *Infection, Genetics and Evolution*, (2010)10: p. 284-291.
- Leon-Sicairos, C.R., Leon-Felix, J., and Arroyo, R., *Microbiol.*, (2004)150: p. 1131-1138.
- Arroyo, R., et al., *Molecular Microbiology*, (1993)7: p. 299-309.
- Eide, D. and Guerinot, M.L., *ASM News*, (1997)63: p. 199-205.
- Hurt, J.A., et al., *J. of Cell Biol.*, (2009)185: p. 265-277.
- Zhao, H., et al., *J. Biol. Chem.*, (1998)273: p. 28713-28720.
- Vega Robledo, G.B., Carrero, J.C., and Ortiz-Ortiz, L., *Parasitol. Res.*, (1999)85: p. 487-492.
- Franco, E., Araujo Soares, M., and Meza, I., *Arch. Med. Res.*, (1999)30: p. 82-88.
- De Jesus, J.B., et al., *Proteomics*, (2007)7: p. 1961-1972.
- Delanote, V., Vandekerckhove, J., and Gettemans, J., *Acta Pharmacologica Sinica*, (2005)26: p. 769-779.
- Kubler, E. and Riezman, H., *Embo J*, (1993)12: p. 2855-2862.
- Adams, A.E.M., Botstein, D., and Drubin, D.G., *Nature*, (1991)354: p.
- Sandrock, T.M., et al., *Genetics*, (1999)151: p. 1287-1297.
- Bozner, P. and Demes, P., *Parasitology*, (1990)102: p.
- Lehker, M.W., et al., *J. Exp. Med.*, (1990)171: p.
- Wolfgang, M., Yuan, L., *Chem. Rev.*, (2009)109: p. 4682-4707.
- Fair, W.R. and Cordonnier, J.J., *J. Urology*, (1978)120: p. 695-698.
- Fiori, P.L., et al., *FEMS Microbiol. Lett.*, (1993)109: p. 13-18.
- Fiori, P.L., et al., *Infect. Immun.*, (1997)65: p. 5142-5148.
- Garber, G.E., Lemchuk-Favel, L.T., and Bowie, W.R., *J. Clin. Microbiol.*, (1989)27: p. 1548-1555.
- Solano-Gonzalez, E., et al., *FEBS Letters*, (2007)581: p. 2919-2928.
- Torres-Romero, J.C., Arroyo, R., *Infection, Genetics and Evolution*, (2009)9: p. 1065-1074.